

Supplementary information to: **Size and property bimodality in magnetic nanoparticle dispersions: Single domain particles vs strongly coupled nanoclusters**

E. Wetterskog^{a}, A. Castro^b, L. Zeng^c, S. Petronis^d, D. Heinke^e, E. Olsson^c, L. Nilsson^{b,f}, N. Gehrke,^e and P. Svedlindh^a*

^a*Solid state physics, Department of Engineering Sciences, Ångström Laboratory, Uppsala University, Sweden, email:
erik.wetterskog@angstrom.uu.se*

^b*SOLVE Research and Consultancy AB, Lund, Sweden*

^c*Department of Applied Physics, Chalmers University of Technology, Göteborg, Sweden*

^d*SP Chemistry, Materials and Surfaces, SP Technical Research Institute of Sweden, Borås, Sweden*

^e*nanoPET Pharma GmbH, Berlin, Germany*

^f*Lund Centre for Field-Flow Fractionation, Department of Food Technology, Engineering and Nutrition, Lund University, Sweden*

ADDITIONAL STRUCTURAL CHARACTERIZATION OF NANOCUSTERS

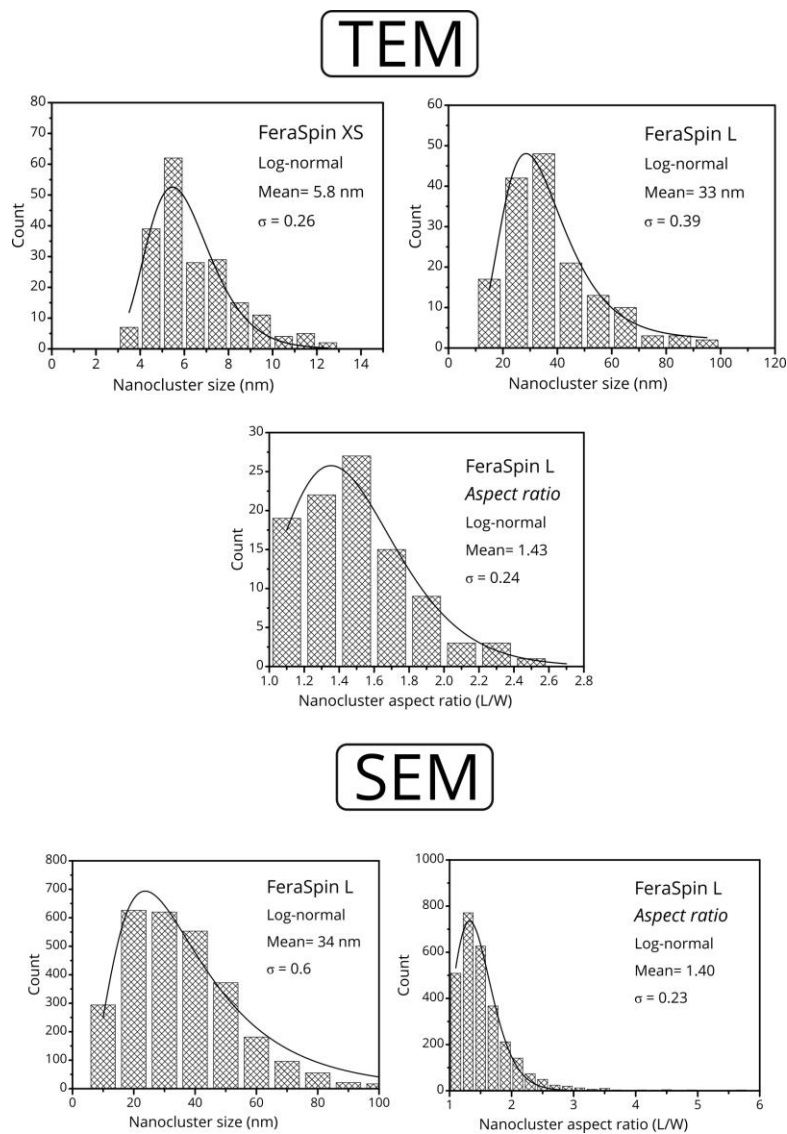


Figure S 1: Histogram of the nanocrystals (FeraSpin XS) and nanocluster (FeraSpin L) sizes, and the aspect ratio (L/W) for FeraSpin L as determined by SEM and TEM.

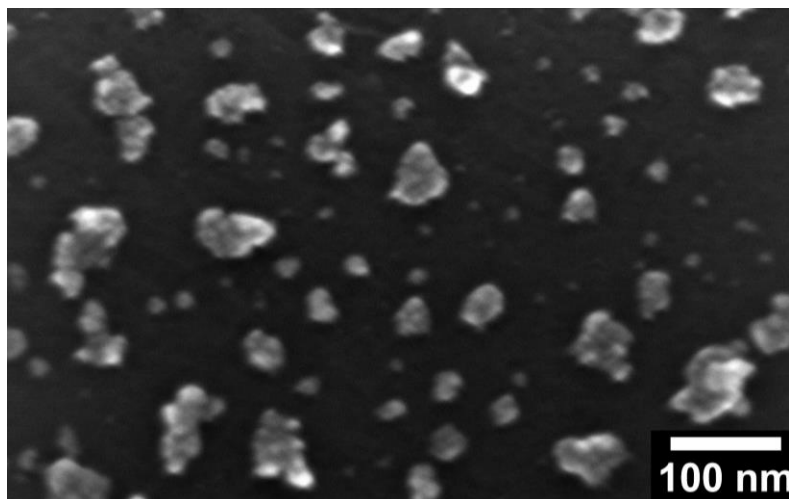


Figure S 2: SEM image of FeraSpin L nanoclusters immobilized on a Si substrate. Please refer to the experimental section for more details on the sample preparation.

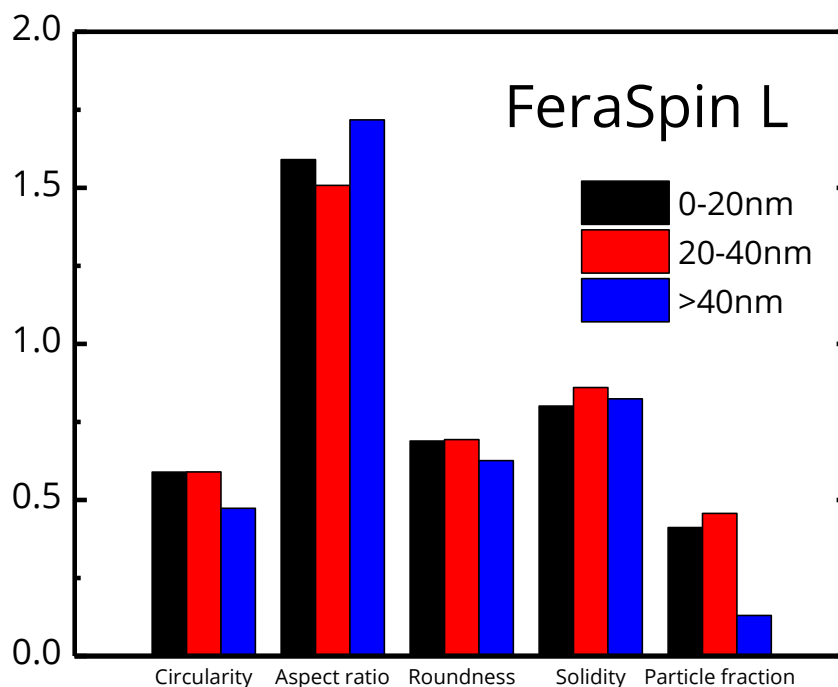


Figure S 3: Particle characteristics for FeraSpin L derived from the SEM analysis using ImageJ, sorted in three different size regimes. Definitions are here as in the documentation of ImageJ. *Aspect ratio*: the aspect ratio of the fitted ellipse to the particle projection, i.e., [Major Axis] / [Minor Axis]. *Roundness*: $(4 \times [\text{Area}]) / (\pi \times [\text{Major axis}]^2)$ or the inverse of [Aspect ratio]. *Solidity*: $[\text{Area}]/[\text{Convex hull area}]$, where convex hull can be thought of as a rubber band wrapped tightly around the projection of the particle. For example, a circle, ellipse, triangle or rectangle would have Solidity = 1, while star- or flower-like shape would have Solidity <1. *Circularity*: $(4\pi \times [\text{Area}])/([\text{Perimeter}]^2)$ with a value of 1.0 indicating a perfect circle. As the value approaches 0.0, it indicates an increasingly elongated shape.

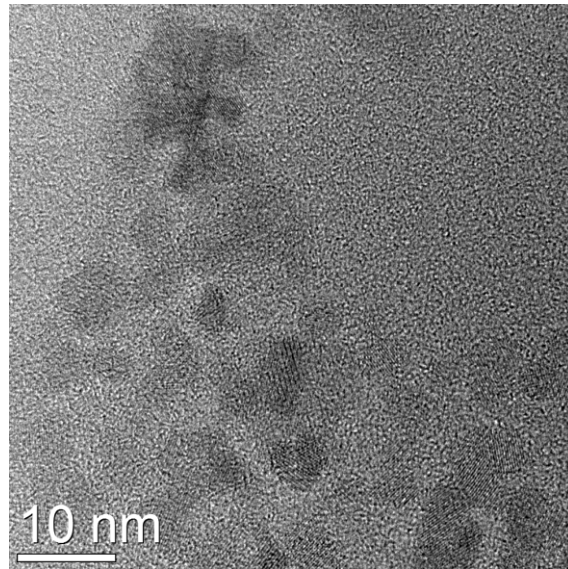


Figure S 4: Soft aggregate in FeraSpin XS, a possible drying artefact during TEM sample preparation. The absence of nanoclusters of larger sizes in the AF4 fractograms, FMR spectra and temperature dependent AC-magnetometry suggest that these agglomerates are either statistically insignificant or formed during de-wetting of the water film evaporation of the dispersion.

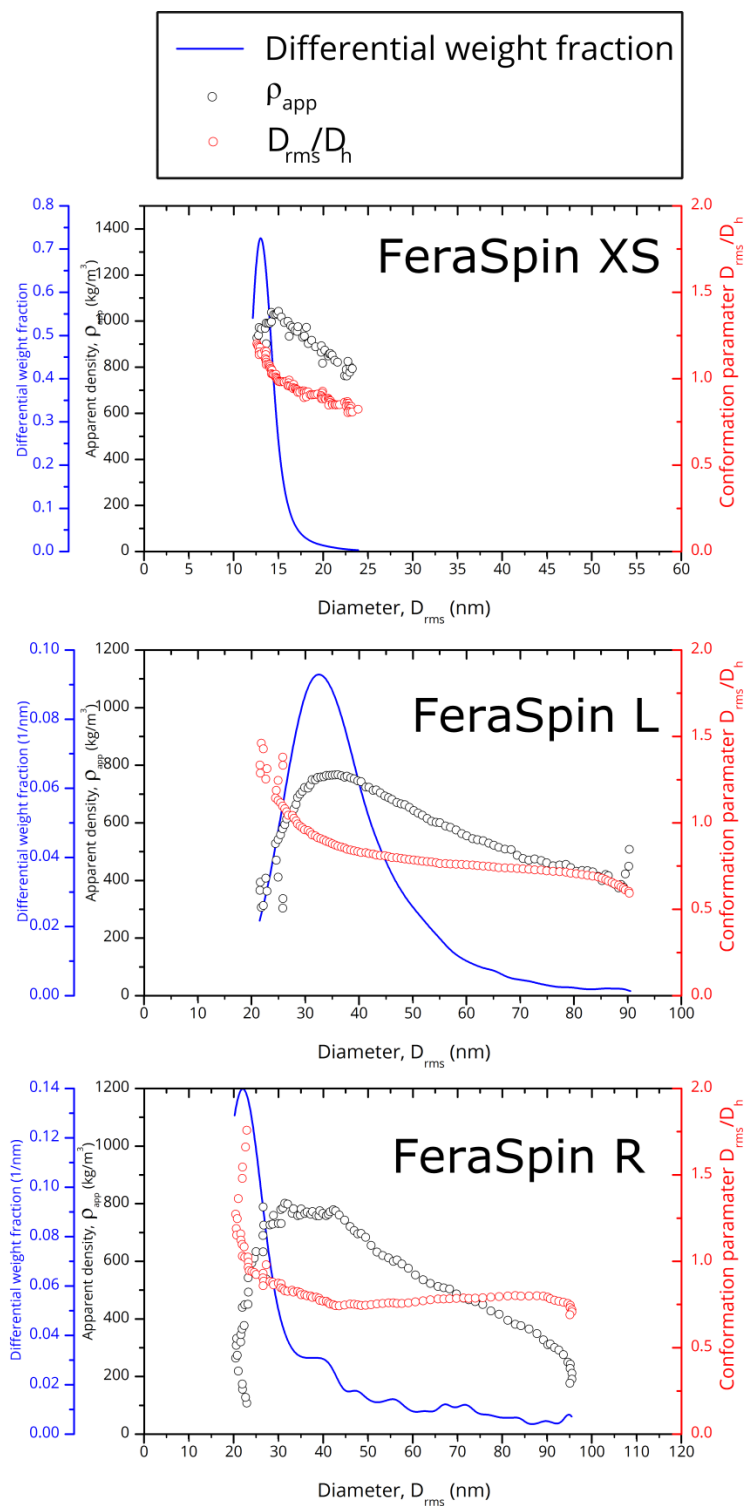


Figure S 5: Differential weight fractions, apparent density (ρ_{app}), and conformational parameter (D_{rms}/D_h) as a function of D_{rms} for dispersions of FeraSpin XS, L, and R.

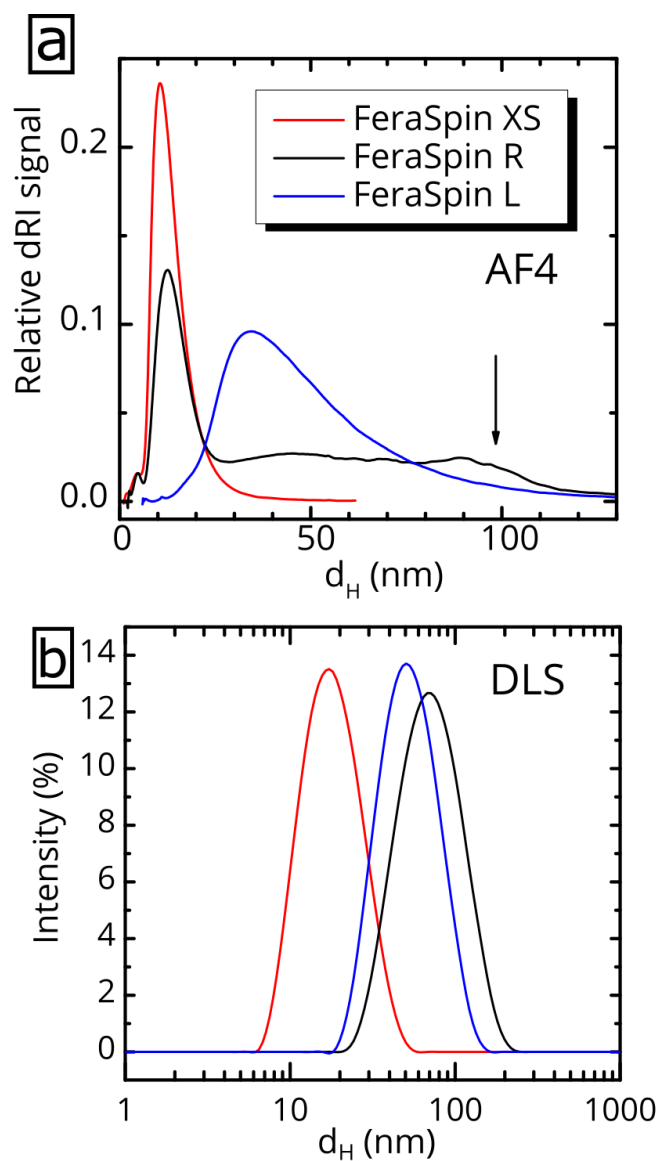


Figure S 6: Comparison of the relative signals of the (a) AF4 refractive index fractograms for the three samples FeraSpin XS, L and R with (b) DLS data. As seen in the figure, FeraSpin R has a longer tail (see arrow) than FeraSpin L, and subsequently has a slightly wider size distribution of colloidal nanoclusters than FeraSpin L.

CALCULATION OF THE DEMAGNETIZATION FACTORS FOR ELLIPSOIDAL PARTICLES

For a general (prolate) ellipsoid with semi-axes $a > b = c$ we have that the components of the demagnetization tensor N are N_{zz} , N_{yy} , N_{zz} (for the semi-axes a , b , c respectively). In general, we have that, $N_{zz} + N_{yy} + N_{xx} = 4\pi$, and when $m = a/c$:

$$\frac{N_{zz}}{4\pi} = \frac{1}{m^2-1} \left(\frac{m}{2\sqrt{(m^2-1)}} \times \ln \left(\frac{m+\sqrt{(m^2-1)}}{m-\sqrt{(m^2-1)}} \right) - 1 \right),$$

$$\frac{N_{xx}}{4\pi} = \frac{N_{yy}}{4\pi} = \frac{m}{2(m^2-1)} \left(m - \frac{1}{2\sqrt{(m^2-1)}} \times \ln \left(\frac{m+\sqrt{(m^2-1)}}{m-\sqrt{(m^2-1)}} \right) \right),$$

The effective demagnetization factor can then be found through $N_{eff} = N_{\perp} - N_{//}$, where $N_{xx} = N_{yy} = N_{\perp} > N_{//} = N_{zz}$. Using a value of $m = \frac{a}{c} = L/W$ (as shown in fig. S1) gives $N_{eff} = 0.13$.

ADDITIONAL FMR DATA

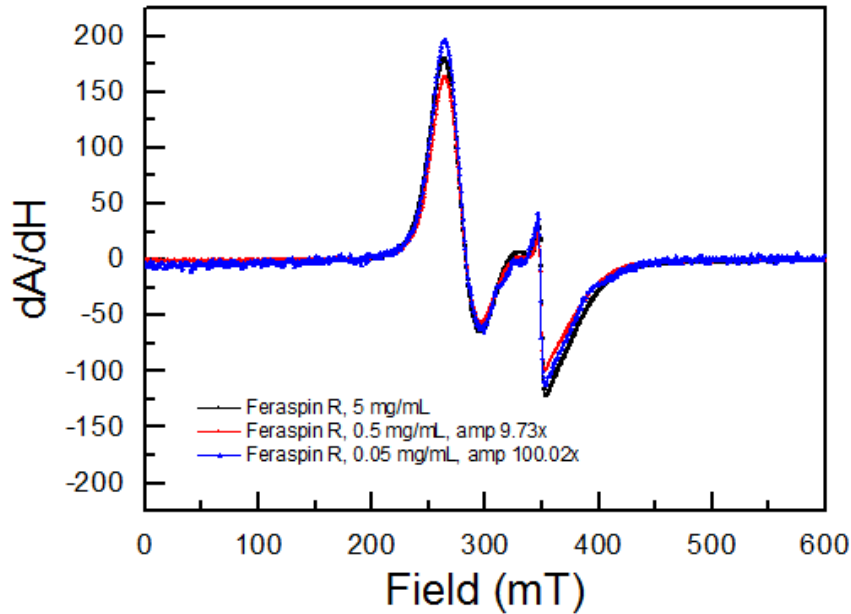


Figure S 7: A concentration series of FeraSpin R diluted $\approx 10x$ and $100x$. The spectra have been renormalized according to the actual dilution factor, determined by weight. Although the data is rather noisy, there are no obvious concentration effects seen after renormalization.

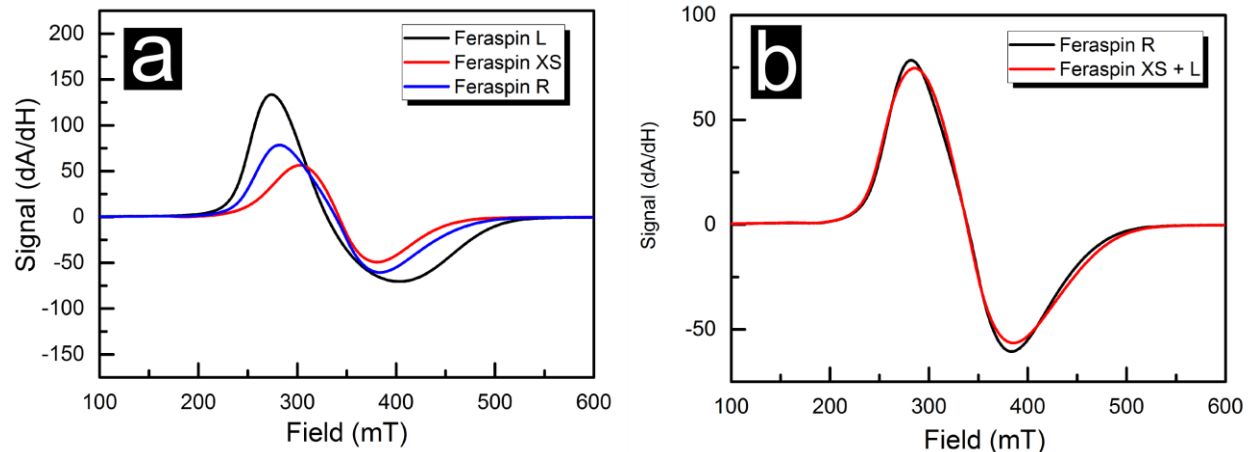


Figure S 8: Additional FMR spectra of immobilized particles. (a) FeraSpin XS, R and L adsorbed in cotton wool. (b) Linear combination fit of the FeraSpin XS + L spectra to the FeraSpin R spectrum.

ADDITIONAL MAGNETIZATION DATA

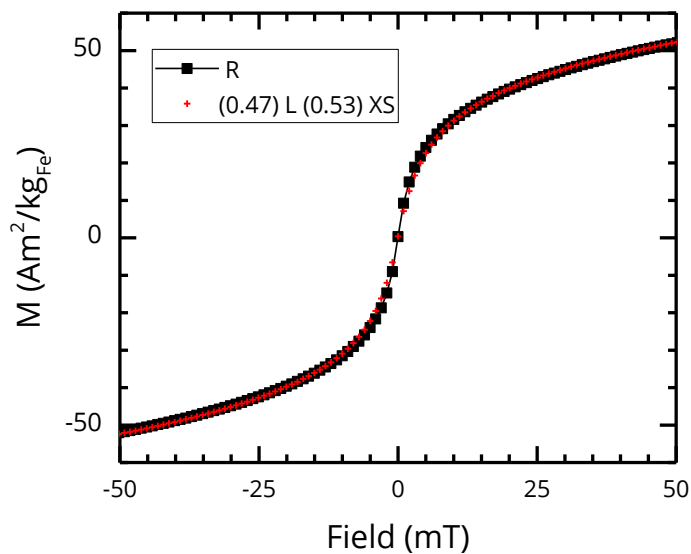


Figure S 9: Fit of the FeraSpin R magnetization (M vs. H) curve using a linear combination of the magnetization curves of FeraSpin XS and FeraSpin L. As seen in the graph, there is a slight mismatch between the original and composite curves in the low-field (< 10 mT) region.

Table S 1: Calculation of K_{eff} using the intra-well potential approximation given in the main paper (eq. 1). Other approximations used are $\rho = 5 \text{ g/cm}^3$ and $m(\text{Fe})/m(\text{Fe}_x\text{O}_y) = 0.7$ (valid for $\gamma\text{-Fe}_2\text{O}_3$). We estimated errors assuming an error in the magnetic moment of 3%.

Sample	$M_s(0)$	Fitted $\chi^{\perp T \rightarrow 0}$ <i>dimensionless</i> <i>SI units</i>	Effective anisotropy <i>AC ($\chi^{\perp T \rightarrow 0}$)</i> <i>$10^4 \text{ J/m}^3$</i>
FeraSpin XS	110 Am ² /kg _{Fe} 385 kA/m	2.25	2.8(2)
FeraSpin L	120 Am ² /kg _{Fe} 420 kA/m	3.50	2.1(2)